THE AMERICAN MINERALOGIST, VOL. 53, MAY–JUNE, 1968

THE CHARACTERIZATION OF BERYL AND EMERALD BY VISIBLE AND INFRARED ABSORPTION SPECTROSCOPY

D. L. WOOD AND K. NASSAU, *Bell Telephone Laboratories, Incorporated, Murray Hill, New Jersey*

ABSTRACT

Absorption measurements with polarized radiation in the visible, ultraviolet, and infrared regions make possible a study of the centers responsible for the differences among various types of beryl. The spectra of two types of water can be recognized with molecular vibrational fundamentals at 1542 $cm^{-1}(\omega)$, 3555 $cm^{-1}(\omega)$ and 3694 $cm^{-1}(\epsilon)$ for Type I, and at 1628 $cm^{-1}(\epsilon)$, 3592 $cm^{-1}(\epsilon)$, and 3655 $cm^{-1}(\omega)$ for Type II. Many overtones and combinations of these fundamentals also have been identified. The Type I molecule is oriented in the channels with its C_2 symmetry axis perpendicular to the crystal C_6-axis, while the Type II molecule is rotated 90° by the action of a nearby alkali ion on the molecular electric dipole. Synthetic flux grown beryl contains no water, and hydrothermal beryl grown in the absence of alkali shows only the Type I spectra. Molecules of CO_2 also are sometimes present in the channels, producing a vibrational absorption frequency of 2353 cm^{-1} (4.25 μ) in the ordinary ray.

Green beryl (emerald) is colored by the Cr^{3+} ion in octahedral Al^{3+} sites, giving rise to the broad bands at 4300 Å and 6000 Å and sharp lines at 4760 Å, 6800 Å and 6830 Å. These features can be accounted for in detail by the crystal field theory, and a nondestructive analysis for Cr^{3+} is possible from a measurement of the intensity of absorption. Chrome-free "emeralds," although deep green in color, have a somewhat different absorption spectrum which can be attributed to octahedral V^{3+} substituted in the Al^{3+} sites. Pale green, blue, or yellow beryls are colored according to the relative intensities of three spectral features attributable to iron ions: (a) a broad band in the extraordinary ray at 6200 Å due to Fe^{2+} in a channel site, (b) an absorption edge near 4000 Å in both ω and ϵ due to octahedral Fe^{3+} in the Al^{3+} site, and (c) narrow bands in both ω and ϵ at 4650 Å and 3740 Å due to Fe^{3+} in tetrahedral Si^{4+} sites. Two other features, also attributable to iron, do not produce any visible coloration: (d) a broad band at 8100 Å in the ordinary ray due to Fe^{2+} in the octahedral Al^{3+} site, and (e) a set of broad components in the extraordinary ray centered around 8100 Å due to Fe^{2+} in a different channel site. These spectral features are interpreted on the basis of the crystal field theory. For pink beryl, the color is due to Mn^{2+}, not Mn^{3+}, but the four component bands in the spectrum at 3550 Å(ϵ), 4950 Å(ω), 5400 Å(ω) and 5550 Å(ϵ) could not be positively identified with the expected crystal field transitions.

INTRODUCTION

Beryl shows a number of characteristic absorption lines or bands in the optically transparent region ranging approximately from 0.25 micron (40,000 cm^{-1}). The colors of the various types of beryls (including aquamarine, golden beryl, morganite, emerald, etc). originate from absorptions in the 0.4 to 0.7 micron range, the causative agents being chromophoric transition metal ions. In the region beyond 4.5 microns there are absorptions due to vibrations of the crystal lattice, the so-called lattice modes. Finally, in the region from about 1 to 7 microns, there are absorptions originating from impurity molecules trapped in the

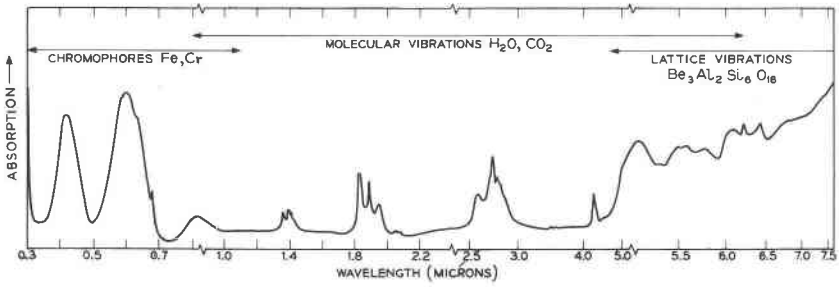

FIG. 1. Composite spectrum of beryl showing: the region of lattice vibrations (4.5μ toward longer wavelength), the region of molecular vibrations (water and CO_2 from 0.84μ to 6.5μ), and the region of chromophoric absorptions (0.3 to 1.1μ), with ordinary ray polarization.

beryl channels. In Figure 1 is shown a composite spectrum illustrating the various regions with specific assignments.

Unpolarized room temperature absorption spectra of beryl have been reported before but we have extended these measurements to include data made with oriented sections, polarized radiation, and low temperatures, so that we are able to extend the interpretation of these spectra in terms of the energy levels of the chromophoric ions. We also review here the importance of the spectra of molecular species in the understanding of the structural details of beryl.

EXPERIMENTAL

Specimens of beryl were obtained from a variety of sources, including commercial dealers, museums, private collections, and from various individuals. A list of the 79 crystals studied is presented in Table I which also gives the origin and spectral characters of the group of crystals. Plane sections were cut and polished with the optic axis parallel to the polished surfaces so that the ordinary (ω) and extraordinary (ϵ) ray spectra could be obtained from the single section by the use of polarized radiation. The orientation was conveniently accomplished by centering the optic normal figure in a polarizing microscope using monochromatic illumination. Spectra were recorded in the ultraviolet-visible-near infrared range on a Cary model 14 double beam spectrophotometer, and in the farther infrared with a Perkin-Elmer model 421 double beam grating spectrophotometer.

THE STRUCTURE AND THE SYNTHESIS OF BERYL

The beryl structure (Bragg and West, 1926; Belov and Matveeva, 1950) consists of a series of SiO_4 and BeO_4 tetrahedra connected with AlO_6

TABLE 1. BERYL SAMPLES STUDIED

1. Synthetic crystals (Emeralds) (with Cr)
   a) Without water (show only lattice modes and Cr lines)

309*	Chatham[a] (flux)	440*	BTL[c] flux grown
413	Chatham (flux)	450	Gilson[a] flux grown
414	Chatham (flux)	476	Chatham (flux)
436	Nacken[b] (flux)	484*	BTL flux grown
437	Nacken (flux)	508	Gilson flux grown
438	Nacken (flux)	509	Gilson flux grown
439*	Nacken (flux)	510	Gilson flux grown

   b) With water (show lattice modes, water type I, and Cr lines)

435*	Linde[a] hydrothermal
457	Linde hydrothermal
485	Lechleitner[a] hydrothermal

2. Natural crystals
   a) Colorless (goshenite) (show lattice modes, water types I and II, some show CO_2, some show Fe^{2+})

375	Mt. Antero, Colo.	481	Erongo Mts., S. W. Africa
430	Unknown	483	Newry, Maine
431	Unknown	503	Unknown
432**	Unknown	1309	Acworth, N. H.
433**	Unknown	10,202	Musinka, Siberia
443**	Brazil	10,297	Stoneham, Me.
444*	Brazil	10,345	Pala, San Diego Co., Cal.
445**	Brazil	18,818a	Minas Geraes, Brazil
446**	Brazil	24,119b	Erongo Mts., S. W. Africa
451*	Unknown	24,119c	Erongo Mts., S. W. Africa

   b) Pale blue or green beryls (aquamarine) (show lattice modes, water types I and II, Fe^{2+}, Fe^{3+}, some show CO_2)

434*	Brazil	505	Unknown
448**	Madagascar	506	Unknown
480	N. Carolina	10,228	Audon-Tschilon, Siberia
486	Brazil	19,813	Klein Spitzkopje, S. W. Africa
504	Unknown	512	Ural Mts., Russia
		513*	Elba, Italy[d]

   c) Dark green beryls (emerald) (show lattice modes, water types I and II, Cr^{3+}, some show Fe^{3+})

415	Colombia	450d	Colombia
416a	Colombia	450e	Colombia
416b	Colombia	477	Brazil
416c	Colombia	478a	Brazil
416d	Colombia	478b	Brazil
449	Brazil	2379a	Colombia
450a	Colombia	2379b	Colombia
450b	Colombia		

   d) Dark green beryls (chromium-free emerald) (show lattice modes, water types I and II, V)

449	Salininha, Brazil
450c	Salininha, Brazil

TABLE 1—(*continued*)

	459a	Salininha, Brazil	
	459b	Salininha, Brazil	
e)	Yellow to brown beryls (heliodor) (show lattice modes, water types I and II, Fe^{2+} Fe^{3+}, some show CO_2)		
	477**	Brazil	514a Nertschinsk, Russia
	29,611	Perm, Russia	514b Nertschinsk, Russia
f)	Pink beryls (morganite) (show lattice modes, water types I and II, Mn)		
	452	Unknown	490 Brazil
	487	Brazil	491 Brazil
	488	Brazil	507 Unknown
	489	Brazil	515 Madagascar

[a] The synthetic techniques are summarized by Flanigen et al. (1967).

[b] Nacken used both hydrothermal (Van Praagh, 1947) and flux (Foerst, 1955) techniques; our Nacken crystals are surely flux grown.

[c] Linares *et al.* (1962).

[d] Vorobyeveite (Rosterite), containing 0.17% Cs, 0.05% Na, and 0.02% Li.

* CO_2 line absent.

** CO_2 line present.

octahedra in the ratio of 6:3:2 to give the composition $Be_3Al_2Si_6O_{18}$. All the silicon tetrahedra occur in rings with hexagonal symmetry stacked above each other in a staggered arrangement producing channels enclosing the *c*-axes. This is shown in the unit cell projection of Figure 2 looking

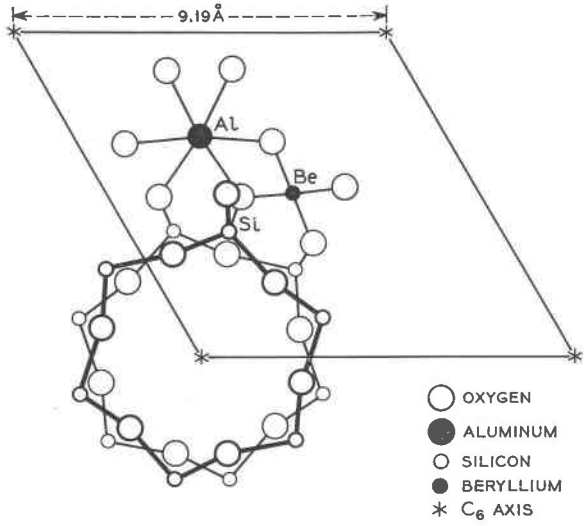

FIG. 2. Projection of part of the structure of beryl on a plane perpendicular to the *c* axis.

down the hexagonal *c*-axis. The beryllium tetrahedra and aluminum octahedra connect the rings together. Figure 3 shows a partial projected cross-section of the oxygen walls of one of the channels.

Based on the ionic radii of Table 2, it is clear that except perhaps for Li^+, alkali ions would be expected to enter only the hexagonal channels. This has, in fact, been demonstrated in the case of Cs^+ by Evans and Mrose (1966). The presence of channel alkali ions is made possible be-

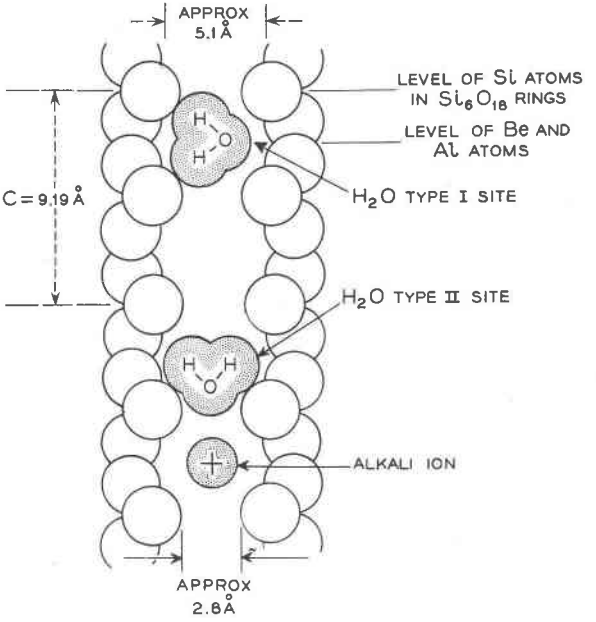

FIG. 3. Partial cross-section of the channels in beryl showing two types of molecular water sites. The crystal *c* axis is vertical in the diagram.

cause of missing negative charges in the lattice produced, for example, by the substitution of Fe^{2+} for Al^{3+} or by the omission of a Be^{2+} ion. Smaller impurity ions such as Fe^{3+} and Cr^{3+} are expected to substitute in the Al site on the basis of ionic radius. Various substitutions, some quite complex, have been suggested, but usually with no evidence other than that they are consistent with overall stoichiometry (Folinsbee, 1941; Deer *et al.*, 1962).

There are two major types of synthetic beryls, one produced by hydrothermal growth and the other from the flux. The hydrothermal technique, approximating closely the growth process occurring in nature, has been used by Nacken (Van Praagh, 1947), Wyart and Sčávincăr (1957), Van

Valkenburg and Weir (1957), and by Flanigen *et al.*, (1965, 1967); the last group of authors did not use any alkali in its syntheses.

Several flux techniques have been used. Fluxes have usually been based on molybdenum oxide (Hautefeuille and Perry, 1888; Espig, 1960; Lefever *et al.*, 1962, used also by Nacken (Forest, 1955)), or on vanadium oxide (Hautefeuille and Perry, 1888; Linares *et al.*, 1962; Linares, 1967).

Commercially available synthetic hydrothermal emeralds include the Linde product (Flanigen *et al.*, 1965, 1967) (solid growth on a thin seed) and the Lechleitner (thin overgrowth on a faceted natural beryl stone). Flux-grown synthetic emeralds prepared by undisclosed processes include the Chatham, Gilson and Zerfass products. Based on the absence of

TABLE 2. DIMENSIONS OF RELEVANCE TO THE BERYL STRUCTURE

(ionic radii in Å)

Lattice ions		Channel sites	
Be^{2+} 0.35		Radius at silicate ring level 1.4 Å	
Al^{3+} 0.51		Radius between rings 2.5 Å	
Si^{4+} 0.42			
Transition ions		**Alkali ions**	**Molecules (effective overall dimensions)**
Mn^{2+} 0.80	V^{5+} 0.59	Li^{+} 0.68	H_2O 2.8×3.2×3.7 Å
Fe^{2+} 0.74	V^{4+} 0.63	Na^{+} 0.94	CO_2 2.8×2.8×5.0 Å
Fe^{3+} 0.64	V^{3+} 0.74	K^{+} 1.33	
Cr^{3+} 0.63	V^{2+} 0.95	Rb^{+} 1.48	
		Cs^{+} 1.67	

water (see below) and the occasional presence of lithium and molybdenum, the "Chatham created" emerald appears to be grown from a lithium molybdate-type flux. Synthetic products are extremely useful in spectroscopic studies since they provide reference material of known composition and growth conditions.

LATTICE VIBRATIONS AND CARBON DIOXIDE

From 4.5μ on into the infrared are found a series of absorptions which are present in all beryl specimens. These are best seen in synthetic flux-grown specimens, (Fig. 4a) which have no other absorptions in this region. These absorptions arise from overtones and combinations of a number of frequencies originating in the vibrations of atoms and groups of atoms of the beryl structure. Well-recognized fundamental vibrations not shown in Figure 4 include the principal SiO_4 bands at 8.2μ and 10.4μ

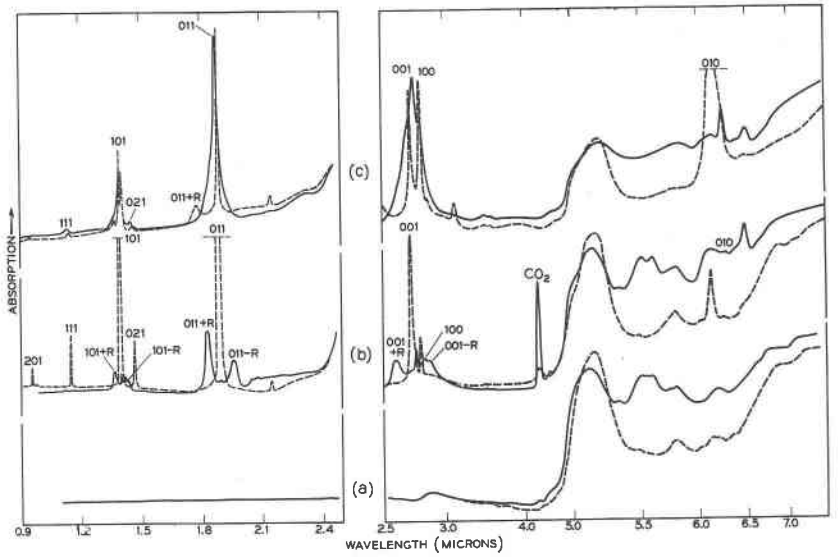

FIG. 4. Absorption spectra of three beryl crystals in polarized radiation, identifying the lines due to water and CO_2: (a) Flux grown synthetic crystal (#309, Chatham) with no molecular lines, absorption bands due to $Be_3Al_2Si_6O_{18}$ only; (b) Spectrum of natural crystal #445 having very nearly all Type I water sites and a strong CO_2 line; (c) Spectrum of natural crystal #489 having mostly Type II water sites. Identification of the site lines follows Wood and Nassau (1967), with the vibrational quantum numbers (ν_1, ν_2, ν_3); Sum and difference lines involving rotational frequencies are identified in addition as pure vibration $+R$ or $-R$, respectively. Dashed lines, extraordinary ray; full lines, ordinary ray.

and a band at 12.5 μ originating in the hexagonal silicate rings (Schaeffer *et al.*, 1934; Plyusnina and Bakii, 1958; Saksena, 1961; Plyusnina, 1963). The intensities of the combinations and overtones decrease with decreasing wavelength and they become unimportant below about 4.5 μ in thin samples. Plyusnina (1964) has described changes in the silicate group vibrations caused by distortions due to the presence of alkali ions.

We have observed a strongly dichroic line at 4.25 μ which is present in many naturally occurring beryls, but not in synthetic ones. This line can be seen in Figure 4b, and the presence or absence of this line is also indicated for some of the specimens listed in Table 1. We have attributed this line to the presence of carbon dioxide molecules based on the close agreement with the unsymmetrical stretching frequency of gaseous CO_2 at 4.26 μ and the presence of sufficient CO_2 in the crystals to account for the intensity (Wood and Nassau, 1967). Since the line is strongly dichroic with greater absorption for the ordinary ray, the CO_2 must be oriented

within the beryl structure and cannot be merely physically trapped in voids. Both CO and CO_2 had been reported previously when beryl was heated (Böse, 1936) but the presence in the lattice was not established. CO_2 has also been reported recently for the closely related mineral cordierite by Farrell and Newnham (1967) and a similar infrared spectrum has been observed.

The linear CO_2 molecule is approximately 5 Å long and 2.8 Å across, so there is adequate room for it in the channels between the silicate rings. Based on the dichroism, the molecule is oriented with its length perpendicular to the C_6 axis (Wood and Nasasu, 1967). Confirmation of the presence of CO_2 was obtained by heating two specimens showing this line, free of any occlusions visible under the micrscope, to 1300°C. Both CO and CO_2 were detected by mass-spectrometry in addition to water and hydrogen in the evolved gas. The CO and hydrogen may have been produced by the reduction of CO_2 and H_2O in contact with the molybdenum crucible used. We estimate that the amount of structural CO_2 present in these channels is at least 0.1 percent by weight. In addition to the CO_2, CO, H_2, and the H_2O discussed below, other molecules reported in the literature to be obtained by heating beryl are He, A, N_2, H_2S and CH_4, (Böse, 1936; Aldritch and Nier, 1948). In the absence of clear-cut evidence such as dichroic absorption bands, one cannot positively locate such molecules within the structure as distinct from physical entrapment by inclusion in voids and cracks.

Water Spectra

The occurrence of water in beryl in the form of free molecules has long been recognized. A detailed study by Wickersheim and Buchanan (1959) demonstrated that varying amounts of more than one type of spectrum were involved. One of these spectra (crystal #3) was interpreted as possibly demonstrating OH^- (Wickersheim and Buchanan, 1959; Wickersheim and Buchanan, 1965), but was subsequently recognized as not being beryl (Wickersheim and Buchanan, 1968).

We have examined 17 synthetic and 62 naturally occurring beryl crystals summarized in Table 1 and from the spectra can comment on the occurrence of various types of water spectra.

Water spectrum, Type I. All the naturally occurring beryls in our collection gave an infrared spectrum which was termed water Type I. The intensity of this spectrum varied from one crystal to another, but extremes were rare. This spectrum is also observed in the Linde hydrothermally grown emerald which is known to be free of alkali. We have identified the 16 lines in this spectrum as belonging to water molecules

aligned with the molecular symmetry axis perpendicular to the hexagonal C_6 axis and the *H-H* direction parallel to the C_6 axis (Wood and Nassau, 1967) as shown in Figure 3. The fundamental vibrations are the deformation ν_2 at 1542 cm^{-1} with perpendicular polarization in the crystal (ordinary ray), the symmetric stretching ν_1 at 3555 cm^{-1} also with perpendicular polarization, and the asymmetric stretching ν_3 at 3694 cm^{-1} with parallel polarization (extraordinary ray).

The assignments of the fundamental and the various combination bands of Type I water are included with the spectrum in Figure 4b recorded from a natural beryl, #445 from Brazil. An ω-polarized combining frequency (Wickersheim and Buchanan, 1965) of 170 cm^{-1} is observed on each side of the ϵ-polarized lines and the low frequency component disappears at 4.2°K (Wood and Nassau, 1967). This is interpreted as a more or less "free" rotation or libration of the water molecules. There is little shift in this combining frequency on lowering the temperature, so that the suggestion that many rotational levels are involved (Boutin *et al.*, 1965) cannot apply. The Type I water appears to be present at least to some extent in all the natural beryl spectra we have seen in the literature.

Water spectrum, Type II. We have observed a second type of spectrum (Wood and Nassau, 1967) termed Water Type II, which is present in many of the naturally occurring beryls, but in greatly varying intensity. For the lowest concentration specimen (#445) it was essentially absent, and this was also true of all the synthetic beryls tested. The strongest Water Type II spectrum observed was in crystal #489, the spectrum of which is shown in Figure 4c.

All the lines in the spectrum of Type II water can be identified as belonging to water molecules aligned with the molecular symmetry axis parallel to the hexagonal C_6 axis as shown in Figure 3. Here the fundamental vibrations are the deformation ν_2 at 1628 cm^{-1} with ϵ-polarization in the crystal, the symmetrical stretching ν_1, at 3592 cm^{-1} also with ϵ-polarization, and the asymmetric stretching ν_3 at 3655 with ω polarization. The assignment of the fundamentals and the various combinations are included in Figure 4c, where the designations for the Type I water bands are omitted for clarity.

We have also shown (Wood and Nassau, 1967) that the intensity of the type II water spectrum increases as the amount of alkali present in the beryl increases, and this has been interpreted in terms relating to the results of Bakakin and Belov (1952) and of Feklichev (1963). The Type II spectrum arises from water molecules which are adjacent to alkali metal ions in the channel, and they are rotated from the perpendicular

to the parallel position by the electric field of the charged alkali ion. As expected, the tighter binding due to the charged alkali ion produces a higher rotational combining frequency in the Type II spectrum; the deformation frequency ν_2 is also raised slightly, undoubtedly reflecting a closer approach of the water protons to the walls of the channel in this spectrum (Wood and Nassau, 1967).

Location of the water molecules. The infrared spectrophotometric results are consistent with the location of the water molecules in the channels and between the silicate rings as Feklichev (1963) concluded. It is difficult to accept the proposal of Bakakin and Belov (1962) that the water molecules are within the rings because of their size. The water molecule is irregular in shape but is not less than 2.8 Å in one plane and 3.2 Å to 3.7 Å in the others. Since the void within the ring has a diameter of about 2.8 Å, the fit would be so tight as to drastically modify the water molecular frequencies. Such a modification is not observed, and we believe that the water is located between the rings. This is supported by recent X-ray studies by Gibbs (unpublished results) and by Vorma *et al.*, (1965).

The Type II spectrum then arises from water molecules between the rings but with an alkali ion nearby to rotate the molecular dipole and produce dichroism opposite to that of the Type I spectrum.

Vorma *et al.*, (1955) and Evans and Mrose (1966) have suggested that the alkali ions are also located between the rings in the same position as the water molecules and at the level of Be and Al ions. This would require that the orienting effect of the alkali ion on Type II water molecules should extend over 4.6 Å, and, if an alkali ion occurred with an H_2O molecule on each side, both would give the Type II spectrum. The intensity ratio of Type I and Type II H_2O absorption bands would then depend on the statistical distribution of alkali ions and water molecules in the channels. We have not attempted to evaluate the alkali position or distribution on the basis of the spectra since we feel that neither the analyses nor the assumptions about the alkali distribution are sufficiently reliable to make a quantitative interpretation meaningful. Our qualitative results do not conflict with those cited above, and we tentatively accept the conclusion that the alkali and the water are both in the positions between the rings. As Evans and Mrose (1966) have shown, Cs^+ ions fit closely in the voids; one would expect Li^+ ions to take uncentered positions along the walls of the void because of their small size. An uncentered alkali ion would be expected to give a slightly different Type II H_2O spectrum than a centered one but no evidence for this has been found.

Binding of the water molecules. It would be natural to speculate that, since the Type I water is bound in the voids between the rings with the H-H line parallel to the channel axis, the binding force must be due to hydrogen bonding with the oxygen ions of the silicate rings. This is inconsistent, however, with the infrared spectrum since hydrogen bonding is known to drastically shift the OH stretching frequencies (Rundle and Parasol, 1952; Lord and Merrifield, 1953) and no such shift is observed. It must be concluded that the silicate oxygen atoms are mostly covalently bonded, and that the orienting forces on the Type I molecule are due to more remote electrostatic charge distributions.

Another factor favoring unbonded water molecules in the Type I site is the following. If the structure of the channel is examined closely, one finds that a water molecule just fits with one H-atom next to the oxygen of one silicate ion in the ring above, and the other H-atom next to the oxygen of a silicate ion in the ring below the water molecule. These oxygen ions are rotated slightly with respect to each other, with a line through their centers making an angle of approximately 18° with the C_6 axis. If the water molecule were hydrogen bonded to these likely looking sites, it then would have its *H-H* axis inclined to the crystal C_6 axis by the same 18°. The dichroic ratio of more than 25 to 1 observed in the absorption lines of the Type I site, however, requires that the *H-H* line be at an angle smaller than 4° to the C_6 axis of the crystal, so that this model of the water site involving hydrogen bonding cannot be correct.

A number of attempts were made to modify the beryl infrared spectra by various treatments. Heating of crystal #446 produced a weight loss of 1.6 percent near 900°C, but #443 did not give off gases even at 1200°C and it still retained the water infrared bands after this treatment. A temperature of 1350°C was necessary to release water and CO_2 from the latter crystal and left a residue which no longer showed any water spectra. This high temperature stability appears to originate from a blocking of the channel by the alkali ions. These ions are presumably quite tightly bound in the immediate neighborhood of the lattice ions for which they provide charge compensation.

The water is liberated gradually during heating, and differential thermal analysis on sample #446 did not show any discontinuities between room temperature and 1000°C. Heating crystal #443 to 1000°C in air, or to 1200°C in vacuum, produced no appreciable changes in the water and CO_2 spectra. The presence of an electric field parallel to the *C* axis during heating did not result in appreciable current flow as it does in the case of quartz (Wenden, 1967; Wood, 1960) nor did it produce any changes in the spectrum. We were unable to introduce water into flux-grown emer-

ald even after 5 days under hydrothermal conditions at 358°C and 8,000 psi since neither the weight nor the spectrum was changed by this treatment. The high stability of beryl with respect to these treatments indicates that the spectra described here can be used with some assurance to evaluate the conditions prevalent during the genesis of crystalline beryl.

The Chromium Spectrum

Beryl, when containing sufficient chromium to color it a strong green (about 0.1% or more), is termed emerald. Whether prepared synthetically (by flux-growth or hydrothermally) or found in nature, essentially the same chromium spectrum is characterized by two broad bands near 4,300 and 6,000 Å, as well as sharp lines at low temperatures (Wood, 1965); one in the blue at 4,760 Å and two in the red at 6,800 and 6,830 Å (the latter lines can also be seen in the room temperature spectra of Figure 5a).

The chromium ions replace the octahedrally coordinated aluminum ions, and this substitution occurs with no charge discrepancy and very little size misfit. According to the structure refinement of Belov and Matveeva (1950), the octahedron is only slightly distorted, and it was necessary in an earlier report (Wood, 1960) to invoke the influence of next nearest neighbors in order to explain the large ground state splitting of the Cr^{3+} ion. It has been found more recently by Gibbs (unpublished results) however, that the octahedron is actually appreciably distorted, and the ground state splitting is probably due entirely to this distortion. The full details of the interpretation of the polarized absorption spectra and their variation with temperature and magnetic field have been reported by one of us (Wood, 1965), where references to earlier work may also be found.

The polarization of the absorption spectrum is the cause of the color change of emerald in polarized light (pleochroism) from yellowish-green for the ordinary ray to bluish-green for the extraordinary ray. The absorption coefficients for crystals of known chromium content have been measured, and it is therefore possible to estimate the concentration in an unknown sample by the nondestructive absorption measurement which has been described in detail for ruby even for unoriented samples (Dodd *et al.*, 1964). If A is the absorbance defined by $A=\log_{10}I_0/I$ for a given polarization of incident light of intensity I_0 and transmitted intensity I, and t the thickness of the sample in cm., then $\alpha=A/t$ is related to the concentration c in weight percent chromium by $\alpha=0.434\ \mu c$. The absorption coefficients μ are given for the ordinary ray and extraordinary ray for emerald in Table 3.

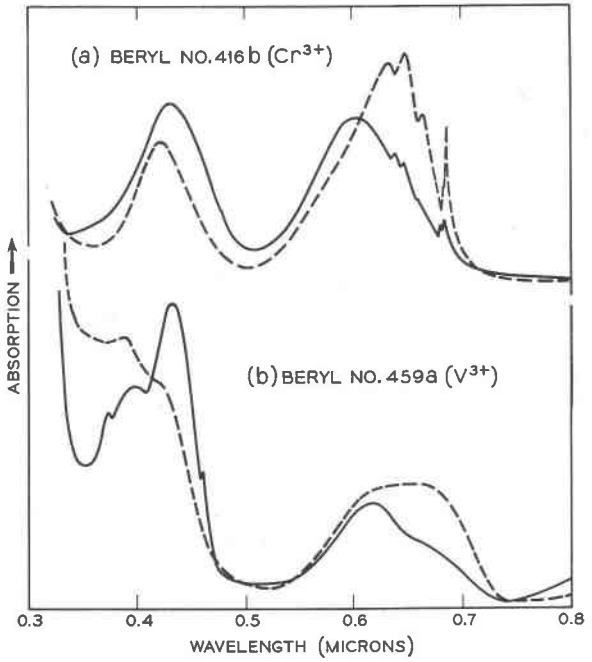

FIG. 5. Spectra of two dark green beryl crystals in the visible region of the spectrum: (a) emerald #416b color due to Cr^{3+} in the Al^{3+} site; (b) chrome-free emerald #459a colored nearly the same but with V^{3+} in the Al^{3+} site. Dashed lines, extraordinary ray; full lines, ordinary ray.

CHROME-FREE EMERALDS

Recently a source of emeralds has been discovered (Selig, 1965) in the state of Bahia in Brazil where beryl of green color very similar to that of "true" emerald is found, but these crystals do not contain sufficient chromium to account for the color (Leiper, 1965; Pough, 1967). From the

TABLE 3. ABSORPTION COEFFICIENTS OF EMERALD

from $1/t \log_{10} I_0/I = 0.434\ \mu c$ with t in cm and c in weight percent chromium

μ, Å	Polarization	μ
4160	ϵ	31
4350	ω	34
5970	ω	31
6300	ϵ	40

absorption coefficients just discussed for chromium in beryl the minimum detectable amount by optical absorption ($\log_{10} I_0/I = 0.05$) or by visual observation of the color in a 2-cm thick piece of material would be 0.0012 percent or 12 ppm. Of course, the minimum concentration to visibly color a crystal less than 2 cm thick would be correspondingly greater than 12 ppm. The analysis reported for the material from Salininha, Bahia, shows one quarter of this amount or 3 ppm (Leiper, 1965). Our analyses for "chrome-free emeralds" also show that the Cr content is less than this minimum detectable amount, and the crystals would be colorless if some other chromophore was not present.

The spectrum of the chrome-free emeralds in the visible region is also different from that for ordinary emeralds as a comparison of Figure 5b with Figure 5a shows. There are two broad bands, one in the red and one in the violet in both spectra, but the frequencies and relative intensities are quite different for the two kinds of crystal. Probably the most important difference is the absence of the sharp *R* lines of chromium which are prominent in the spectrum of ordinary emerald. In a material whose coloration involved both chromium and another chromophore, the presence of these sharp lines would characterize the chromium, while the relative intensities of the broad bands would be different from that of ordinary emerald.

The analyses given in Table 4 show that one element common to all the chrome-free emerald samples is vanadium, and we believe that it is possible to account for the green color on the basis of trivalent vanadium substituted in the Al^{3+} octahedral sites. The crystal field energy levels for this ion are known for Al_2O_3 (McClure, 1962) and for glasses (Kakabadse and Vassiliou, 1965) as well as for solutions (Orgel, 1955) and transitions $^3T_1(^3F) \rightarrow {}^3T_2(^3F)$ and $^3T_1(^3F) \rightarrow {}^3A_2(^3F)$ occur in the visible region. In the case of Al_2O_3 it is known that the crystal field is higher for the Cr^{3+} ion than for the same ion in the octahedral site in beryl (Wood, 1965), and it is safe to assume that the same will be the case for the V^{3+} ion. Thus on this basis one would expect that the crystal field parameter *Dq* would be about 1650 cm^{-1} in beryl, and this would predict from theory (Liehr and Ballhausen, 1959) that the V^{3+} bands would lie at 16,500 cm^{-1} and 24,000 cm^{-1}, which compares favorably with the observed values of 15,300 cm^{+1} and 25,000 cm^{-1}.

The fine structure present in the higher frequency band may be due to the presence of several singlet levels which may mix through spin-orbit coupling with the triplet giving composite levels to which transitions of considerable intensity may take place (Liehr and Ballhausen, 1959). The energy levels of V^{2+}, V^{4+} and V^{5+} are also known for octahedral coordination, and their spectra do not resemble those of Figure 5b.

TABLE 4. EMERALD AND BERYL ANALYSES

Crystal identification	#448 Aquamarine Madagascar	#416a Emerald Muzo	#440 Emerald BTL	#476 Emerald Chatham	#436 Emerald Nacken	#449 CFE[a] Salininha	#450c CFE Salininha	#459a CFE Salininha	#459b CFE Salininha	CFE[b] Bahia
Prin. >10%	Be,Si	Be,Si	Be,Si	Be,Si	Be, Si	Be,Si	Be,Si	Be,Si	Be,Si	Be,Si
Major >1%	Al	Al	Al	Al	Al	Al,Mg	Al,Mg,Na	Al,Mg,Na Ti	Al,Mg,Na Ca	Al,Mg,Na
Minor 0.1–3%		Na			Cr	Na	Fe,V	Ca,Fe,V	Fe,Ti,V	Fe,V
Imp. 0.01–0.3%	Fe,Na,Zn	Cr,Fe, Mg,V	Cr,V	Cr,Mo	V,Mo	Ca,V,Fe	Mn	Mn	Mn	Ca,Ti
Tr. <0.03			Fe	Fe	Fe	Ti	Ca			Sc
Sl. Tr. <0.001	Ca,Cu	Ca,Cu	Mn,Mg,Ca	Li,Mn,Mg,	Mn,Mg	Cu,Mn	Cr,Cu		Cr,Cu	Cr,Ga,Sn
			Ca	Ca	Ca					
V.Sl. Tr. <0.005	Ga,Mg,Mn		Fe,Cu	Cu,V	Cu,Li		Ti	Cr,Cu		Mn,B

[a] CFE stands for Chrome-Free Emerald.

[b] From Leiper (1965).

The fact that vanadium may color beryl green may seem inconsistent with the fact that synthetic beryl grown from a lithium vanadate or V_2O_5 flux is colorless (Linares *et al.*, 1962) but we believe that this is a matter of the valence of the vanadium available to the growing crystal in the flux. If only the colorless pentavalent ion is present in the flux, then it may be accepted into the trivalent sites available only with difficulty. It must require, then, special conditions for the formation of the trivalent vanadium in the flux growth of chrome-free emerald. The fact that all chrome-free emeralds so far examined are very high in alkali and magnesium (Table 4) is not required for the explanation of the color, but it may have importance in the growth conditions establishing the trivalent vanadium ion during the genesis of the crystal. Many chromium containing emeralds show sufficient vanadium content that the origin of their colors should be attributed to both chromium *and* vanadium.

Iron Spectra

Many beryl crystals contain appreciable iron concentrations, and this can impart a blue, green, or yellow color as in aquamarine or heliodor. It may also leave the crystal colorless as in some goshenites, or it may modify the color due to other chromophores. Any variety of beryl, including vorobyeveite characterized by a high Cs content, may exhibit iron colors in addition to their other properties. We have characterized five different spectral features attributable to iron ions, and these can be shown to be independent of each other. The five features are: (1) a strong band at 8100 Å for the ordinary ray, (2) an ϵ-component at the same wavelength, (3) an ϵ-component at 6200 Å, (4) a broad edge absorption near 4000 Å, and (5) line absorptions at 3740 Å and 4650 Å.

6,000 to 8,000 Å region. Most crystals whatever their color have a strong absorption near 8100 Å in the ordinary ray as shown in Figure 6 and this feature has been studied by Grum-Grzhimailo *et al.* (1956, 1962). These workers have attributed the band to the Fe^{2+} ion, and in octahedral coordination this transition would correspond to $^5T_2(^5D) \rightarrow {}^5E(^5D)$ in the low spin configuration (Tanabe and Sugano, 1954). This would be the only spin-allowed transition expected in the spectral region covered, and the energy separation involved implies a crystal field parameter value of $Dq = 1235$ cm^{-1} (Liehr, unpublished results). This is a reasonable value for a divalent 3d transition metal ion with octahedral oxygen coordination (Jørgensen, 1962). It is very unlikely that the transition could arise from tetrahedral Fe^{2+} replacing Be^{2+} or Si^{4+} from the point of view of both the magnitude of Dq and the ionic radius. Tetrahedral Fe^{2+} would be expected to have the transition $^5T_2 \rightarrow {}^5E$ near 6000 cm^{-1} instead of 12,350

cm^{-1} (Tanabe and Sugano, 1954) and Fe^{2+} has an ionic radius of 0.74 Å compared with 0.35 for Be^{2+} and 0.42 Å for Si^{4+}. Thus the nearly octahedral site of Al^{3+} with ionic radius 0.51 Å is the most likely substitutional site for Fe^{2+}. It therefore seems reasonable to attribute this band to $^5T_2 \rightarrow {}^5E$ of octahedral Fe^{2+} substituted for Al^{3+} in the structure.

In some crystals there is also a component of absorption in the extraordinary ray in the same wavelength range, but the ratio of intensity of absorption for ϵ and ω polarizations varies from one crystal to another. Comparison of Figures 6 and 7 shows this to be the case (and Figs. 1 and 2 of Grum-Grzhimailo *et al.*, (1956) confirm it). The ϵ-polarized absorp-

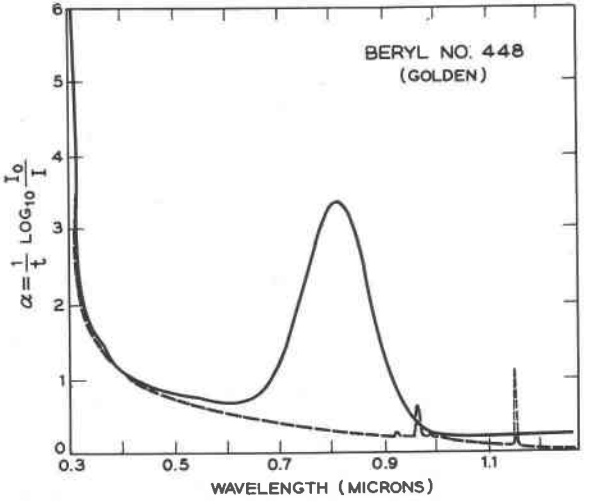

FIG. 6. Absorption spectrum of golden beryl #448: Dashed curve, extraordinary ray; full curve, ordinary ray.

tion therefore arises from a different center than that of the ω-spectrum. The frequency is appropriate to the $^5T_2 \rightarrow {}^5E$ of an Fe^{2+} ion, and because the line is so broad we suggest that the ion responsible is located in the axial channel ways, probably at the level of the rings (Fig. 3) where the ionic distances would be smallest. This would lead to changes in the spectrum if water molecules or alkali ions were nearby, but we have found no definite evidence of such an effect.

The third feature of the iron absorption is the broad band near 6200 Å which is found as a shoulder in the ϵ-spectrum in blue beryls. Such beryls look blue for the extraordinary ray, but yellow or colorless in the ordinary ray because the 6200 Å band removes the red transmitted light. Figure 7 shows how this comes about, and comparison with Figure 8

where the band is absent shows that it is an independent feature. Again because the band is so broad we suggest that it arises from Fe^{2+} in the axial channels, but different from the preceding type, perhaps in a hydrated form. It is certainly not Fe^{3+} or Fe^{2+} in octahedral or tetrahedral sites.

3,000 to 5,000 Å *region.* One of the short wavelength features of the spectra of iron containing beryls is the broad absorption edge from 3200 Å to 4500 Å in Figure 6 which is missing from Figure 8, and which causes

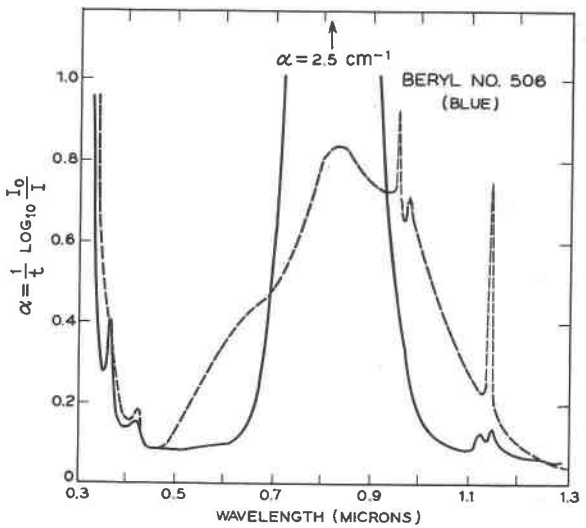

FIG. 7. Absorption spectrum of blue beryl #506. Dashed curve, extraordinary ray; full curve, ordinary ray.

a yellow color when it alone is present. When both the 6200 Å band of blue beryls and the short wavelength absorption edge of yellow beryls are present, the crystal has a greenish color, and all shades between blue and yellow are possible. When both features are absent as in the spectrum of Figure 8, the crystal appears colorless even though the 8100 Å band is very strong. This is because there is essentially no absorption in the region to which the eye is sensitive (~4200 Å to ~6800 Å). The short wavelength edge of Figure 6 can be assigned to Fe^{3+}, not only because ferric salts are usually yellow or brown, but also because of heat treatment experiments whose results are shown in Figure 9. Here a yellow beryl #447 was heated for 16 hours at 520°C in an atmosphere of flowing hydrogen gas. Before this strongly reducing treatment the short wave-

length cut-off was above 4000 Å, and the 8100 Å peaks due to Fe^{2+} were rather weak. After the treatment the short wavelength edge was shifted by a very considerable amount to 3500 Å or below, while the Fe^{2+} absorptions at 8100 Å became more intense in both the ϵ and ω spectra. Heat treatment in air at the same temperature does not change the edge. Thus both the Fe^{3+} short wavelength edge and the 8100 Å Fe^{2+} assignments were confirmed by the decrease of the Fe^{3+} absorption and the increase in Fe^{2+} absorption in the reduced crystal.

The nature of the short wavelength absorption edge of Fe^{3+} in an octahedral site in oxide crystals has been discussed by Clogston (1960), Wickersheim and Lefever (1962), and by Wood and Remeika (1967), and it is generally understood to arise from an allowed charge transfer transition involving the motion of an electron from the O^{2-} ligands to the central metal ion. Because it is a very strong absorption, its presence may be characteristic of only a small fraction of the ferric iron present. On the basis of charge and ionic radius the most likely site is that of the octahedral Al^{3+}, but this evidence is not conclusive.

The last feature of the iron absorption spectrum consists of two lines at 3740 Å and 4650 Å in the ultraviolet and violet regions. These lines presumably arise from crystal field 3d-3d transitions in the ferric ion.

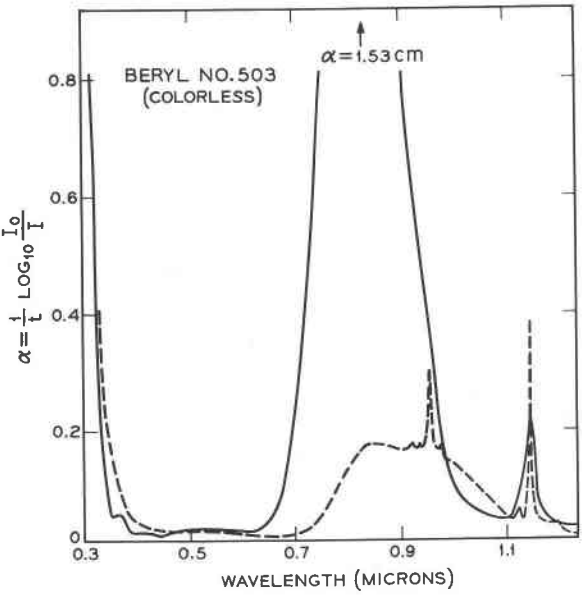

FIG. 8. Absorption spectrum of colorless beryl #503. Dashed curve, extraordinary ray; full curve, ordinary ray.

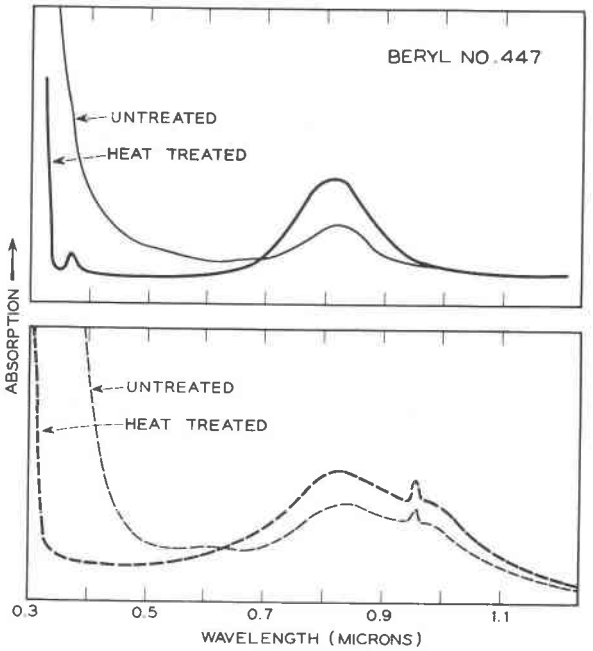

FIG. 9. Changes in the absorption spectrum due to heating golden beryl #447 at 520°C in 1 atmosphere of pure H_2. Dashed curves, extraordinary ray; full curves, ordinary ray.

Because of their high frequency it is likely that they are characteristic of tetrahedrally coordinated Fe^{3+} and correspond to the $^6A_2 \rightarrow {}^4T_1$ (4650 Å) and $^6A_2 \rightarrow {}^4T_2$ (3740 Å) transitions of the $3d^5$ configuration (Liehr and Ballahusen, 1959). On the basis of size alone the Si^{4+} site is more likely, but no conclusive evidence against the Be^{2+} site exists. These Fe^{3+} lines do not contribute color to the crystal; they can be seen in the ω and ϵ spectra of Figure 7.

Because the characteristic absorption coefficients for the various kinds of iron are not known individually, we have not been able to correlate the iron concentration determined by direct analysis with the five spectral features just discussed. Every natural crystal has very likely some of each type of center and probably there is a great disparity of the absorption per ion making the correlation difficult. The five types of iron are summarized in Table 5.

PINK BERYLS

Finally, we would like to add a few comments about pink beryl (Morganite). Analysis shows that all pink crystals in our collection (Table I)

TABLE 5. FIVE TYPES OF IRON IN BERYL

Optical characteristic	Possible assignment	Observed coloration
8100 Å ω broad band, single component	Fe^{2+} in oct. Al site	none
8100 Å ϵ broad band, more than one component	Fe^{2+} in channel site A	none
6200 Å ϵ broad band, single component	Fe^{2+} in channel site B	Blue
4000 Å ω and ϵ edge absorption	Fe^{3+} in oct. Al site	Yellow
3740 Å ω, 4650 Å ω and ϵ, narrow bands	Fe^{3+} in tet. Si site	none

have one foreign element in common, namely manganese. The possibility therefore exists that manganese may be the chromophoric ion. There are at least two likely valence states, Mn^{2+} and Mn^{3+}, and two types of coordination: octahedral when substituted for Al^{3+}, and tetrahedral when substituted for Be^{2+} or Si^{4+}. The observed spectrum with which the transitions in these four possible centers must be reconciled is shown in Figure 10, and four components are discernible at 3550 Å (ϵ), 4950 Å (ω), 5400 Å (ω) and 5550 Å (ϵ) as indicated in the figure. No other absorptions appear to be present. From a knowledge of the Mn^{3+} ($3d^4$) and Mn^{2+} ($3d^5$) crystal-field energy-level diagrams (Tanabe and Sugano, 1954), it is possible to rule out some of these possibilities immediately. For Mn^{3+} one expects a single broad band near 1.4 μ in the near infrared for tetrahedral coordination ($^5T_2 \rightarrow {}^5E$), and a single broad band near

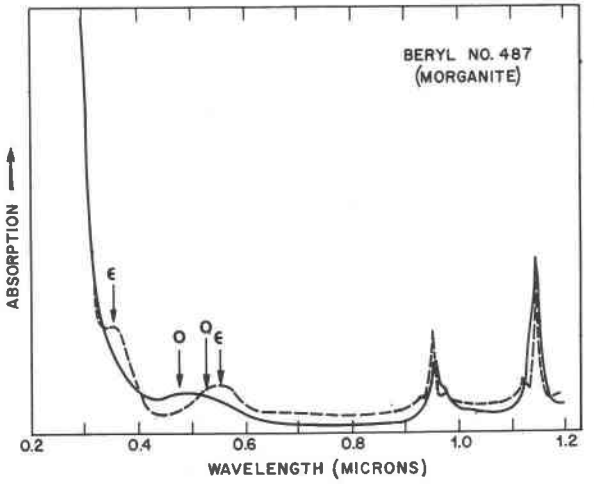

FIG. 10. Absorption spectrum of pink beryl #487. Dashed curve, extraordinary ray; full curve, ordinary ray.

7000 Å for octahedral coordination ($^5E \rightarrow {}^5T_2$). Neither of these fits the observations so that Mn^{3+} can be eliminated.

For Mn^{2+}, on the other hand, one expects three bands near the observed positions for the octahedrally coordinated ion, and a similar set for the tetrahedral ion but at somewhat higher frequency ($^6A_1 \rightarrow {}^4T_1$, $^6A_1 \rightarrow {}^4T_2$, $^6A_1 \rightarrow {}^4A_1$, ^4E). The difficulty with four observed components is removed if the reduced symmetry of the site is considered, but the relative positions of the bands do not agree well with the predictions of crystal field theory. The spacing from the 3550 Å component to the other three is too large for the separation between the 4950 Å and 5550 Å components. It is possible that there is a superposition of more than one type of spectrum in our crystals, including the possibility of ions in the axial voids, and we do not feel confident that a reliable crystal field analysis can be made at this time. We do feel confident, however, that the color is caused by the manganese ion.

ACKNOWLEDGMENT

It is a pleasure to acknowledge the help of the following in obtaining crystals: L. G. Van Vitert, Bell Technical Laboratories; F. H. Pough, V. Manson, of the New York Museum of Natural History; L. Moyd of the National Museum of Canada, Ottawa; J. S. White of the Smithsonian Institution, Washington, D. C., G. R. Crowningshield, R. T. Liddicoat, Jr., and B. Krashes of the Gemological Institute of America; Linde Company, Division of Union Carbide; Created Gemstones, Incorporated; and M. R. Benedict Company. Valuable technical assistance was provided by Miss D. M. Dodd, Miss B. E. Prescott, W. E. Burke, D. L. Nash, E. M. Kelly, and A. J. Caporaso.

REFERENCES

ALDRITCH, L. T. AND A. O. NIER (1948) The occurrence of He^3 in natural sources of helium. *Phys. Rev.*, **74,** 1590–1594.

BAKAKIN, V. V. AND N. V. BELOV (1962) Crystal chemistry of beryl. *Geokhimiya*, 420–433.

BELOV, N. V. AND R. G. MATVEEVA (1950) Determination of the parameters of beryl by the method of partial projection. *Dokl. Akad. Nauk. SSSR*, **73,** 299–302.

BÖSE, R. (1963) Optische und spektrographische Untersuchugen an Beryllen, insbesondere bei höheren Temperaturen. *Neues Jahrb. Mineral, Abt. A, Beilage.* **70,** 467–570.

BOUTIN, H., G. J. SAFFORD AND H. R. DANNER (1965) Low frequency motions of H_2O molecules in crystals. *J. Chem. Phys.*, **42,** 1469–1470.

BRAGG, W. L. AND J. WEST (1926) The structure of beryl, $Be_3Al_2Si_6O_{18}$. *Proc. Roy. Soc. (London)*, A111, 691–714.

CLOGSTON, A. M. (1960) Interaction of magnetic crystals with radiation in the range 10^4–10^5 cm^{-1}. *J. Appl. Phys.*, **31,** 198S–205S.

DEER, W. A., R. A. HOWIE AND J. ZUSSMAN (1962), *Rock-forming Minerals*, Vol. 1, John Wiley & Sons, New York, 256.

DODD, D. M., D. L. WOOD, AND R. L. BARNS (1964) Spectrophotometric determination of chromium concentration in ruby. *J. Appl. Phys.* **35,** 1183–1186.

ESPIG, H. (1960) The synthesis of emeralds. *Chem. Technik*, **12,** 327–331.

EVANS, H. T. JR. AND M. E. MROSE (1966) Crystal chemical studies of cesium beryl (abstr.) *Geol. Soc. Amer. Meet.*, p. 63.

FARRELL, E. F. AND R. E. NEWNHAM (1967) Electronic and vibrational absorption spectra in cordierite. Amer. Mineral. 52, 380–388.

FEKLICHEV, V. G. (1963) Chemical composition of minerals of the beryl group. *Geokhimia* **1963,** 391–401.

FLANIGEN, E. M., D. W. BRECK, N. R. MUMBACH AND A. M. TAYLOR (1965) New hydrothermal emerald. *Gems Gemology*, **11,** 259–264.

———, D. W. BRECK, N. R. MUMBACH AND A. M. TAYLOR (1967) Characteristics of synthetic emeralds. *Amer. Mineral.*, **52,** 744–772.

FOERST, W. (1955) Smaragd-Synthese. *Ullmans Encyclopädie der technischen Chemie* Vol. 6, Urban and Schwarzenberg, Munich-Berlin, p. 246.

FOLINSBEE, R. E. (1954) Optic properties of cordierite in relation to alkalies in the cordierite-beryl structure. *Amer. Mineral.* **26,** 485–500.

GRUM-GRZHIMAILO, S. V., N. A. BRILLIANTOV, R. K. SVIRIDOVA, O. N. Sukhanova and M. M. Kapitonova (1962) Absorption spectra of iron-colored beryls at temperatures from 290 to 1.7°K. *Optics Spectr.*, **13,** 133–134.

——— AND L. A. PEVNEVA (1956) Absorption spectra of colored beryls and topazes. *Trudy Inst. Kristallogr. Akad. Nauk. SSSR*, **12,** 85–192.

HAUTEFEUILLE, P. AND A. PERREY (1888) Sur la reproduction de la phenacite et de l'Emeraude. *C. R. Acad. Sci. Paris.* **106,** 1800–1802.

JORGENSEN, C. K. (1962) *Absorption spectra and chemical bonding in complexes.* Addison-Wesley, Reading, Mass., p. 285.

KAKABADSE, G. J. AND E. VASSILIOU (1965) The isolation of vanadium oxides in glasses. *Phys. Chem. Glasses*, **6,** 33–37.

LEFEVER, R. A., A. B. CHASE AND L. E. SOBON (1962) Synthetic emerald. *Amer. Mineral.* **47,** 1450–1453.

LIEPER, H. N. (1965) Salininha emeralds are definitely shown to have chromium content. *Lapidary J.*, **19,** 990–991.

LIEHR, A. D. AND C. J. BALLAHUSEN (1959) Complete theory of Ni (II) and V(III) in cubic crystalline fields. *Ann. Phys.* **6,** 134–155.

LINARES, R. C. (1967) Growth of beryl from molten salt solutions, *Amer. Mineral.* **52,** 1554–1559.

———, A. A. BALLMAN AND L. G. VAN UITERT (1962) Growth of beryl single crystals for microwave applications. *J. Appl. Phys.*, **33,** 3209–3210.

LORD, R. C. AND R. E. MERRIFIELD (1953) Strong hydrogen bonds in crystals. *J. Chem. Phys.*, **21,** 166–167.

MCCLURE, D. S. (1962) Optical spectra of transition-metal ions in corundum. *J. Chem. Phys.*, **36,** 2757–2779.

ORGEL, L. E. (1955) Spectra of transition-metal complexes. Electronic structures of transition-metal complexes. Band widths in the spectra of manganous and other transition-metal complexes. *J. Chem. Phys.*, 1004–14; 1819–23; 1824–29.

PLYUSNINA, I. I. (1963) Infrared absorption spectra of beryllium minerals. *Geokhimia*, **13,** 158–163.

——— (1964) Infrared absorption spectra of beryls. *Geokhimia*, **14,** 31–41.

——— AND G. B. BAKII (1958) The infrared reflection spectra of the cyclosilicates in the wavelength interval from 7–15 μ. *Sov. Phys. Crystallogr.*, **3,** 761–764.

POUGH, F. H. (1967) Proceedings of the 11th international Gemmological Conference in Barcelona. *Lapidary J.*, **20,** 1268–1277.

RUNDLE, R. E. AND M. PARASOL (1952) OH stretching frequencies in very short and possibly symmetrical hydrogen bonds. *J. Chem. Phys.*, **20,** 1487.

SAKSENA, B. D. (1961) Infrared absorption studies of some silicate structures. *Trans. Faraday Soc.*, **57**, 242–258.

SELIG, B. L. (1965) Caraniba emerald mine. *Gems Minerals*, 22–24.

SCHAEFFER, C., F. MATOSSI AND WIRTZ (1934) Das Ultrarote Reflexionsspeletrum von Silikaten, *Z. Phys.*, **89**, 210–233.

TANABE, Y. AND S. SUGANO (1954) On the absorption spectra of complexions. *J. Phys. Soc. Japan.*, **9**, 766–779.

VAN PRAAGH, G. (1947) Synthetic quartz crystals. *Geol. Mag.*, **84**, 98–99.

VAN VALKENBURG, A. AND C. E. WEIR (1957) Beryl studies $3BeO \cdot Al_2O_3 \cdot 6SiO_2$. (abstr.). *Bull. Geol. Soc. Amer.*, **68**, 1808.

VORMA, A., T. G. SAHAMA AND I. HAAPALA (1965) Alkali position in the beryl structure. *C. R. Soc. Geol. Fin.* **37**, 119–124.

WENDEN, H. E. (1957) Ionic diffusion and the properties of quartz in the direct current resistivity. *Amer. Mineral* **42**, 859–888.

WICKERSHEIM, K. A. AND R. A. BUCHANAN (1959) The near infrared spectrum of beryl. *Amer. Mineral.* **44**, 440–444.

——— AND ——— (1965) Some remarks concerning the spectra of water and hydroxyl groups in beryl. *J. Chem. Phys.*, **42**, 1468–1469.

——— AND ——— (1968) The near infrared spectrum of beryl, a correction. *Amer. Mineral.* **53**, 347.

WOOD, D. L. (1960) Infrared absorption of defects in quartz. *J. Phys. Chem. Solids*, **13**, 326–336.

——— (1965) Absorption fluorescence and Zeeman effect in emerald. *J. Chem. Phys.*, **42**, 3404–3410.

——— AND K. NASSAU (1967) Infrared spectra of foreign molecules in beryl. *J. Chem. Phys.*, **47**, 2220–2228.

——— AND J. P. REMEIKA (1967) Effect of impurities on the optical properties of yttrium iron garnet. *J. Appl. Phys.*, **38**, 1038–1045.

WYART, J. AND S. SCĂVNICĂR (1957) Synthese hydrothermale du beryl. *Bull. Soc. Franc. Mineral. Cristalogr.*, **80**, 395.

Manuscript received, September 11, 1967; accepted for publication, December 15, 1967.